Neuron
Article

Interplay between VGLUT Isoforms and Endophilin A1 Regulates Neurotransmitter Release and Short-Term Plasticity

Matthew C. Weston,[1] Ralf B. Nehring,[1] Sonja M. Wojcik,[2] and Christian Rosenmund[1,3,*]
[1]Departments of Neuroscience and Molecular and Human Genetics, Baylor College of Medicine, Houston, TX 77030, USA
[2]Max-Planck-Institut für Experimentelle Medizin, Abteilung Molekulare Neurobiologie, Hermann-Rein-Strasse 3, D-37075 Göttingen, Germany
[3]NeuroCure Cluster of Excellence, Charité, Universitätsmedizin Berlin, 10115 Berlin, Germany
*Correspondence: christian.rosenmund@charite.de
DOI 10.1016/j.neuron.2011.02.002

SUMMARY

Vesicular glutamate transporters (VGLUTs) are essential for filling synaptic vesicles with glutamate and mammals express three VGLUT isoforms (VGLUT1–3) with distinct spatiotemporal expression patterns. Here, we find that neurons expressing VGLUT1 have lower release probability and less short-term depression than neurons expressing VGLUT2 or VGLUT3. Investigation of the underlying mechanism identified endophilin A1 as a positive regulator of exocytosis whose expression levels are positively correlated with release efficiency and showed that the differences in release efficiency between VGLUT1- and VGLUT2-expressing neurons are due to VGLUT1's ability to bind endophilin A1 and inhibit endophilin-induced enhancement of release probability.

INTRODUCTION

Synapses of the central nervous system display great diversity in functional properties such as quantal size, release probability, and short-term plasticity. These functional properties must be matched to the demands placed upon the synapse and underlying them must be differences in molecular composition. However, there are still few specific examples of how the molecular composition of the presynapse determines its functional properties.

Which neurotransmitter (or neurotransmitters) a synapse releases is determined by expression of the vesicular neurotransmitter transporters. Neurons that release glutamate, the most common excitatory neurotransmitter in the central nervous system, express vesicular glutamate transporters (VGLUTs), which perform the essential function of filling synaptic vesicles with glutamate (Bai et al., 2001; Bellocchio et al., 2000; Fremeau et al., 2001; Schäfer et al., 2002; Takamori et al., 2000, 2001, 2002; Varoqui et al., 2002). In mammals, three VGLUT isoforms have been identified: VGLUT1, VGLUT2, and VGLUT3. However, it is unclear whether each isoform performs a specific function.

Several in vitro studies have reported that the three isoforms show similar transport rates, substrate affinity, and pharmacological profiles, suggesting that the isoforms do not differ in the way they transport glutamate (Bellocchio et al., 2000; Fremeau et al., 2001; Gras et al., 2002; Hayashi et al., 2001; Herzog et al., 2001; Takamori et al., 2000, 2002). Genetic deletion of each gene in mice resulted in a severe reduction in glutamate release from neurons that express that particular isoform, suggesting that they are all necessary for glutamate release from synapses where they are expressed (Fremeau et al., 2004; Moechars et al., 2006; Seal et al., 2008; Wallén-Mackenzie et al., 2006; Wojcik et al., 2004). Upon their initial identification, it was noted that VGLUT1 and VGLUT2 mRNA expression correlated with the probability of neurotransmitter release (Fremeau et al., 2001; Liu, 2003), but there has been no evidence supporting a causal role for VGLUTs in regulating release probability.

The expression patterns of VGLUT mRNAs in the brain, however, are spatially and temporally distinct (Boulland et al., 2004; Kaneko and Fujiyama, 2002; Nakamura et al., 2005), suggesting a specialized function for each isoform. VGLUT1 is present in neurons of the cerebral cortex, hippocampus, and cerebellar cortex and has a late onset of expression, but VGLUT2 is expressed in early development and at its highest levels in the thalamus and lower brainstem regions of adult rodents (Herzog et al., 2001; Kaneko et al., 2002). VGLUT1 and VGLUT2 are the most abundant isoforms and account for most neurons previously thought to release glutamate. VGLUT3 is found in hair cells of the auditory pathway, where it is essential for glutamate release (Gillespie et al., 2005; Obholzer et al., 2008; Ruel et al., 2008; Seal et al., 2008), as well as in pain-sensing neurons of the dorsal root ganglion (Seal et al., 2009). It is also present in neurons that release other neurotransmitters such as GABA, acetylcholine, and serotonin, where it serves to enhance the filling of serotonin and acetylcholine (Amilhon et al., 2010; Gras et al., 2002, 2008; Herzog et al., 2004). Thus, the specific expression patterns of VGLUT1, VGLUT2, and VGLUT3 suggest that each isoform may play a specialized role in glutamate release.

We therefore decided to test the hypothesis that the three VGLUT isoforms confer specific properties of glutamatergic neurotransmission upon the synapses at which they are present.

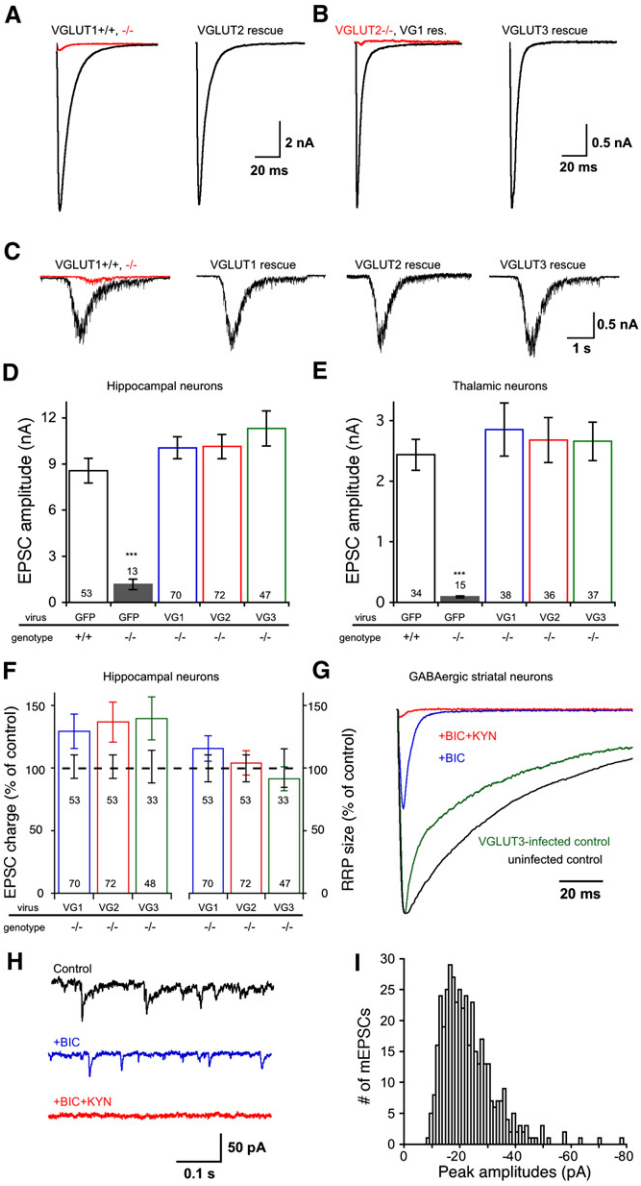

Figure 1. Exogenous VGLUT1, VGLUT2, or VGLUT3 Expression Rescues Deficits in *VGLUT–/–* Neurons

(A) Representative EPSC traces from *VGLUT1*+/+ (black) and *VGLUT1*−/− (red) hippocampal neurons (left traces) and a *VGLUT1*−/− neuron infected with a VGLUT2-expressing lentivirus (right trace) in response to 2 ms depolarizations.

(B) Representative EPSC traces from a VGLUT2−/− thalamic neuron (red) and a *VGLUT2*−/− thalamic neuron infected with a VGLUT1-expressing lentivirus (black, left traces) and a *VGLUT2*−/− thalamic neuron infected with a VGLUT3-expressing lentivirus (right trace) in response to 2 ms depolarizations.

(C) Responses of *VGLUT1*+/+ (black) and *VGLUT1*−/− (red) hippocampal neurons to 4 s application of 500 mM sucrose (left traces) with responses of *VGLUT1*−/− hippocampal neurons infected with a lentivirus expressing VGLUT1, VGLUT2, and VGLUT3.

(D) Bar graph showing the peak EPSC amplitudes of *VGLUT1*+/+, *VGLUT1*−/−, and *VGLUT1*−/− hippocampal neurons rescued with VGLUT1, VGLUT2, or VGLUT3 in response to 2 ms depolarization (mean ± SEM). ***p ≤ 0.001.

We used whole-cell voltage clamp to record synaptic currents from primary cultured neurons expressing different endogenous or virally expressed VGLUT isoforms and measured basic parameters of synaptic function. Our results demonstrate that expression of any VGLUT, including VGLUT3, gives a neuron the ability to release glutamate and that neurons expressing VGLUT1 exhibit lower vesicular release probability (P_{vr}) and altered short-term plasticity compared to VGLUT2- or VGLUT3-expressing neurons. In exploring the mechanism by which VGLUT isoforms regulate exocytosis, we identified endophilin A1 as a positive regulator of release efficiency and propose that VGLUT1's effects result from binding and inhibiting endophilin A1.

RESULTS

VGLUT1, VGLUT2, and VGLUT3 Rescue the EPSC and RRP of Hippocampal *VGLUT1–/–* and Thalamic *VGLUT2–/–* Neurons

We wanted to directly compare the basic functions of VGLUT1, VGLUT2 and VGLUT3 in an otherwise identical cellular environment. Previous studies demonstrated that hippocampal *VGLUT1*−/− neurons and thalamic *VGLUT2*−/− neurons have very low or undetectable levels of VGLUT protein, virtually no evoked or spontaneous glutamate release, and a very small readily releasable pool (RRP) of filled synaptic vesicles (Fremeau et al., 2004; Moechars et al., 2006; Wojcik et al., 2004). We prepared primary autaptic cultures of these neurons and used lentiviruses to induce expression of each of the three VGLUT isoforms. We then performed whole-cell voltage-clamp analysis to test for rescue of the synaptic response.

Evoked responses were measured in knockout neurons and neurons infected with VGLUT1, VGLUT2, and VGLUT3-expressing lentiviruses. Expression of all three isoforms rescued the deficit in EPSC peak amplitude and EPSC charge in both *VGLUT1*−/− hippocampal neurons (Figures 1A and 1D) and

(E) Bar graph showing the peak EPSC amplitudes of *VGLUT2*+/+, *VGLUT2*−/−, and *VGLUT2*−/− thalamic neurons rescued with either VGLUT1, VGLUT2, or VGLUT3 in response to 2 ms depolarization (mean ± SEM). ***p ≤ 0.001.

(F) Bar graph showing the charge contained in the EPSC of *VGLUT1*−/− hippocampal neurons rescued with VGLUT1, VGLUT2, or VGLUT3 (left bars) and the charge contained in the readily releasable pool (RRP) as measured by the charge transfer in response to a 4 s application of 500 mM sucrose (right bars). Values are normalized to littermate *VGLUT*+/+ neurons represented by the black dashed line (mean ± SEM). Numbers in bars graphs are n values.

(G) Representative traces from a GABAergic striatal control neuron (black trace) and a neuron infected with VGLUT3-expressing lentivirus (green trace) recorded with 136 mM Cl^- internal solution. Amplitudes are normalized to the peak amplitude of each control response. Application of 30 μM bicuculline (BIC) (blue trace) reveals a fast-decaying glutamatergic component of the response that is confirmed by application of bicuculline and kynurenic acid (KYN, 3 mM) (red trace).

(H) Representative traces of spontaneous release in a VGLUT3 infected striatal cell. The control trace (black) shows slowly decaying mIPSCs. Blockade of GABA receptors with BIC isolates mEPSCs (blue trace) and application of both BIC and KYN (red trace) blocks spontaneous release.

(I) Cumulative amplitude distribution of mEPSCs recorded from three VGLUT3-expressing GABAergic striatal neurons.

VGLUT2−/− thalamic neurons (Figures 1B and 1E). The EPSC amplitudes of neurons rescued with VGLUT1, VGLUT2 and VGLUT3 were not significantly different from hippocampal *VGLUT*+/+ neurons infected with a lentivirus expressing only GFP, nor were they significantly different from each other (Figures 1D and 1E). The charge contained in the EPSC of VGLUT1, VGLUT2 and VGLUT3 expressing hippocampal neurons were slightly larger, but not significantly different from, control neurons, and were not significantly different from each other (Figure 1F, left panel). We also measured the size of the charge contained in the RRP by applying 500 mM sucrose (Rosenmund and Stevens, 1996). Again all three VGLUT isoforms rescued the severe deficit seen in both *VGLUT1*−/− hippocampal neurons (Figures 1C and 1F) and *VGLUT2*−/− thalamic neurons (data not shown) to levels not significantly different from *VGLUT*+/+ thalamic neurons, suggesting that the three isoforms perform the basic function of filling synaptic vesicles with glutamate in a similar manner.

VGLUT3 Is Sufficient for Glutamate Release in GABAergic Cells

Because VGLUT3 is expressed mainly in neurons thought to release other classical neurotransmitters, we decided to test whether expression of VGLUT3 in nonglutamatergic cells was sufficient for synaptic glutamate release. We prepared primary cultures of GABAergic striatal neurons and infected them with the VGLUT3-expressing lentivirus. We measured synaptic responses with high Cl^--containing internal solution and isolated the glutamatergic component of the synaptic response with bicuculline (30 μM) and/or kynurenic acid (3 mM). As previously shown for VGLUT1 and VGLUT2 (Takamori et al., 2000, 2001), VGLUT3 expressed in GABAergic striatal neurons was sufficient to induce glutamate release in these cells that normally release only GABA (Figure 1G). After 14 days in vitro, glutamatergic EPSC were recorded in 21 of 28 infected neurons, while no glutamatergic EPSCs were recorded from uninfected control GABAergic neurons (n = 15).

In addition to the analysis of evoked release, we tested whether spontaneous release of glutamate could be detected in these neurons. Blocking GABA receptors with bicuculline (30 μM) in infected neurons revealed mEPSCs that were blocked by kynurenic acid (3 mM, Figure 1H) and had peak amplitudes that were similar to glutamatergic neurons (Figure 1I; Moechars et al., 2006), suggesting that the transport and accumulation of glutamate by VGLUT3 in synaptic vesicles of neurons that release neurotransmitters other than glutamate is similar to transport in native glutamatergic neurons, and that VGLUT3 expression is sufficient for a glutamatergic phenotype in central neurons.

VGLUT1, VGLUT2, and VGLUT3 Have Distinct Effects on P_{vr} and Short-Term Plasticity

Because neurons that express VGLUT1 and VGLUT2 in vivo show a correlation between the isoform expressed and probability of glutamate release (Fremeau et al., 2001; Liu, 2003), we performed an analysis of P_{vr} and short-term plasticity in order to determine whether neurons with different VGLUT isoforms release glutamate in quantitatively distinct manners. We first examined cell types in which VGLUT1 and VGLUT2 are differentially expressed in vivo. For VGLUT1 expressing cells we chose hippocampal neurons, in which 85%–90% of the excitatory synaptic current depends on VGLUT1 (Fremeau et al., 2004; Wojcik et al., 2004). For VGLUT2 we chose thalamic neurons, in which 90% of the excitatory synaptic response depends on VGLUT2 (Moechars et al., 2006). We calculated the P_{vr} by comparing the charge contained in the RRP with the charge of the EPSC. Thalamic neurons had a significantly higher P_{vr} than hippocampal neurons and showed strong paired-pulse depression characteristic of high-release probability synapses. In contrast, hippocampal neurons showed moderate paired-pulse facilitation and lower P_{vr} (Figures 2A and 2B). In addition, application of high-frequency stimulation (10 Hz) caused EPSCs of thalamic neurons to depress to only 20% of their prestimulus values after 5 s, while hippocampal neurons were able to maintain EPSC amplitudes averaging approximately 60% of prestimulus values (data not shown).

The analysis of wild-type hippocampal and thalamic neurons demonstrates that VGLUT isoform expression correlates with properties of glutamate release. It does not, however, demonstrate a causal relationship, because numerous other differences between hippocampal and thalamic neurons may influence their P_{vr} and short-term plasticity. We therefore returned to the knockout-rescue approach to allow a direct comparison of the VGLUTs in an identical cellular environment. Analysis of P_{vr} revealed that hippocampal *VGLUT1*−/− neurons rescued with VGLUT1 had a P_{vr} identical to hippocampal *VGLUT1*+/+ neurons. However, when either VGLUT2 or VGLUT3 was expressed in the *VGLUT1*−/− hippocampal neurons, release probabilities increased 30%–35% relative to both *VGLUT1*+/+ and VGLUT1 rescue neurons (Figure 2D). In addition, rescue with the endogenous isoform VGLUT1 produced neurons with paired-pulse facilitation, while VGLUT2-expressing neurons showed paired-pulse depression (Figures 2C and 2F, VGLUT3 not tested). Consistent with this finding, the response to high-frequency stimulation of *VGLUT1*−/− neurons expressing VGLUT1 was indistinguishable from *VGLUT1*+/+ neurons, while VGLUT2 and VGLUT3-expressing neurons showed significantly more depression (Figure 2E), indicating higher release probability in the latter two groups.

In order to test whether the effect of VGLUT expression on P_{vr} was specific to hippocampal cells, we repeated the analysis by expressing VGLUT1 and VGLUT2 in thalamic *VGLUT2*−/− neurons. In thalamic *VGLUT2*−/− cells, rescue with VGLUT2 produced neurons with P_{vr} that were indistinguishable from thalamic *VGLUT2*+/+ neurons, while neurons rescued with VGLUT1 showed a significant 25% reduction (Figure 2H). Paired-pulse ratios were also significantly different between VGLUT1- and VGLUT2-expressing cells (Figure 2G). Depression in response to 10 Hz stimulation was slightly greater in VGLUT2-expressing neurons than VGLUT1-expressing neurons, but not significantly different, as both types still displayed the near complete depletion characteristic of thalamic cells (data not shown).

It is important to note that although expression of VGLUT2 in hippocampal neurons was sufficient to induce a thalamic-like phenotype, while expression of VGLUT1 in thalamic neurons

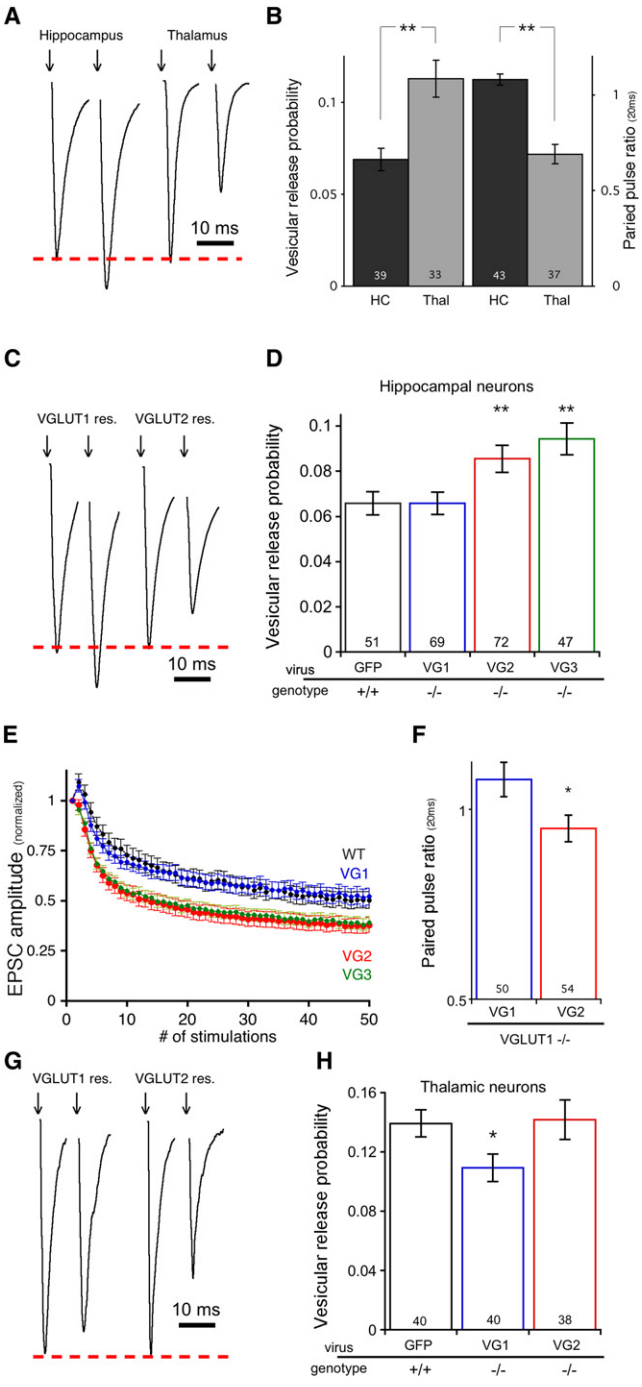

Figure 2. VGLUT Isoforms Control Vesicular Release Probability (P_{vr}) and Short-Term Plasticity

(A) Representative traces of primary autaptic cultured hippocampal (left trace) and thalamic (right trace) neurons in response to two brief (2 ms) depolarizations separated by 20 ms. The somatic current is blanked for display purposes. Arrows indicate time of stimulation.

(B) Bar graph showing the P_{vr} (left bars) and the 20 ms paired-pulse ratio (right bars) of hippocampal and thalamic neurons. P_{vr} was calculated by the fraction of the RRP released per EPSC. The paired-pulse ratio was calculated by the peak amplitude of the second response divided by the peak amplitude of the first.

induced a hippocampal-like phenotype, the effects were not strong enough to completely account for the differences between the wild-type hippocampal and thalamic neurons. We also note that the changes in P_{vr} were not accompanied by significant differences in either of the component parameters, EPSC charge or RRP size. Both EPSC charge and RRP size are, however, heavily dependent on the number of synapses formed by the neurons, which can vary by neuron, culture, and age of culture, while P_{vr} is not affected by synapse number.

Differences in Release Probability Are Not Due to VGLUT Expression Levels at the Synapse

Having established that VGLUT1-expressing neurons release glutamate with a lower probability than VGLUT2- and VGLUT3-expressing neurons, we wanted to investigate possible mechanisms. Because VGLUT isoforms may differ in their trafficking (Fremeau et al., 2001) and variable levels of VGLUT protein at the synapse may affect P_{vr} and short-term plasticity, we first performed a quantitative analysis of immunofluorescent images to compare expression levels of VGLUT1 and VGLUT2 at the synapse (Figure S1, available online). After electrophysiology experiments were completed we immunostained the remaining neurons for VGLUT1, VGLUT2, and synaptophysin (Figure S1A). We then compared the ratio of VGLUT fluorescence intensity to the vesicular protein synaptophysin fluorescence intensity at identified synapses (De Gois et al., 2005; Wilson et al., 2005). Both *VGLUT1*−/− and *VGLUT1*+/− neurons showed a significant reduction in VGLUT/synaptophysin fluorescence ratio compared to *VGLUT1*+/+, while overexpression of VGLUT1 showed a significant increase (Figure S1B). VGLUT/synaptophysin fluorescence ratios in *VGLUT1*−/− neurons infected with VGLUT1, however, were not different from *VGLUT1*+/+ neurons (Figure S1B). To compare expression levels of VGLUT1 and VGLUT2 proteins we inserted a myc tag into the first luminal loop of each transporter to circumvent the complications of different primary antibody affinities. These constructs were first tested with electrophysiology in neurons to confirm they retained the phenotypes of the untagged VGLUTs (data not shown). The cultures

(C) Representative paired-pulse EPSC traces from *VGLUT1*−/− hippocampal neurons infected with a VGLUT1-expressing lentivirus (left trace) or a VGLUT2-expressing lentivirus (right trace).

(D) Bar graph showing the P_{vr} measured from *VGLUT1*+/+ and *VGLUT1*−/− hippocampal neurons rescued with VGLUT1, VGLUT2, or VGLUT3 (mean ± SEM).

(E) Line plot of the responses of *VGLUT1*+/+ and *VGLUT1*−/− hippocampal neurons rescued with VGLUT1, VGLUT2, or VGLUT3 (mean ± SEM) to 10 Hz stimulation. Values are normalized to the peak amplitude of the first response in the train.

(F) Bar graph showing the paired-pulse ratios (mean ± SEM, 20 ms interstimulus interval) measured in *VGLUT1*−/− hippocampal neurons expressing VGLUT1 or VGLUT2.

(G) Representative paired-pulse EPSC traces from *VGLUT2*−/− thalamic neurons infected with a VGLUT1-expressing lentivirus (left trace) or a VGLUT2-expressing lentivirus (right trace).

(H) Bar graph showing the P_{vr} measured from *VGLUT2*+/+ and *VGLUT2*−/− thalamic neurons rescued with VGLUT1 or VGLUT2 (mean ± SEM). For all bar graphs *$p \leq 0.05$, **$p \leq 0.01$. See Experimental Procedures for statistical details. Numbers in bars are n values.

were then fixed and immunostained with anti-myc and anti-synaptophysin antibodies. The myc/synaptophysin intensity ratios in *VGLUT*−/− neurons expressing either VGLUT1-myc or VGLUT2-myc were not different from each other (Figure S1C), demonstrating that the differences in P_{vr} and paired-pulse ratios in these neurons were not due to different expression levels at the synapse.

No Differences in mEPSC Parameters or RRP Refilling

Next, we considered that the VGLUT isoforms might induce different filling states of synaptic vesicles, which may alter the probability of glutamate release (Moechars et al., 2006; Wilson et al., 2005; Wojcik et al., 2004). We therefore tested whether the observed differences in P_{vr} and paired-pulse ratio between VGLUT isoforms correlated with mEPSC amplitude. As previously reported, *VGLUT1*−/− neurons showed a significant reduction in mEPSC amplitude and overexpression of VGLUT1 in *VGLUT1*+/+ neurons resulted in significantly larger mEPSC amplitudes compared to *VGLUT1*+/+ (Wilson et al., 2005; Wojcik et al., 2004; Figures 3A and 3B). Expression of VGLUT1, VGLUT2, or VGLUT3 in *VGLUT*−/− neurons, however, resulted in mEPSC amplitudes that were indistinguishable from *VGLUT1*+/+ (Figures 3A and 3B), suggesting that the lower release probability and altered short-term plasticity of VGLUT1-expressing neurons is not due to fewer numbers of transporters on synaptic vesicles or lower levels of glutamate in the vesicles. mEPSC frequency was also measured and no significant differences were found between *VGLUT1*+/+ neurons and any of the constructs tested (Figure 3C).

We performed two additional analyses to rule out other possible mechanisms. First we examined the shape of the mEPSC as an indicator of postsynaptic receptor subunit changes and found no difference in the amplitude to charge ratio of mEPSCs from VGLUT1-, VGLUT2-, or VGLUT3-expressing neurons (Figure 3D). Finally, we examined the rate of refilling of the RRP by depleting the RRP with one 500 mM sucrose application, followed by a second application 5 s later. There were no differences in the percentage of the RRP refilled after 5 s between any of the groups (Figure 3E).

Mutating the VGLUT1-Endophilin Binding Site Abolishes Differences in P_{vr} and Short-Term Plasticity

Finally we considered that a differential protein-protein interaction might underlie the differences between VGLUT isoforms. The most striking difference between VGLUT1 and VGLUT2/3 that has been reported so far is the existence of the polyproline motif on the C terminus of VGLUT1 that mediates an interaction with endophilins (De Gois et al., 2006; Vinatier et al., 2006; Voglmaier et al., 2006), a protein family primarily known for its role in synaptic vesicle endocytosis (Farsad et al., 2001; Guichet et al., 2002; Hill et al., 2001; Ringstad et al., 1999; Schmidt et al., 1999; Schuske et al., 2003; Simpson et al., 1999). Both VGLUT2 and VGLUT3 lack this motif. We therefore expressed VGLUT1 containing a point mutation shown to disrupt endophilin binding (P554A) (Vinatier et al., 2006) in *VGLUT1*−/− hippocampal cells and repeated the measurements of P_{vr}, paired-pulse ratio, and 10 Hz stimulation with VGLUT1- and VGLUT2-rescued cells.

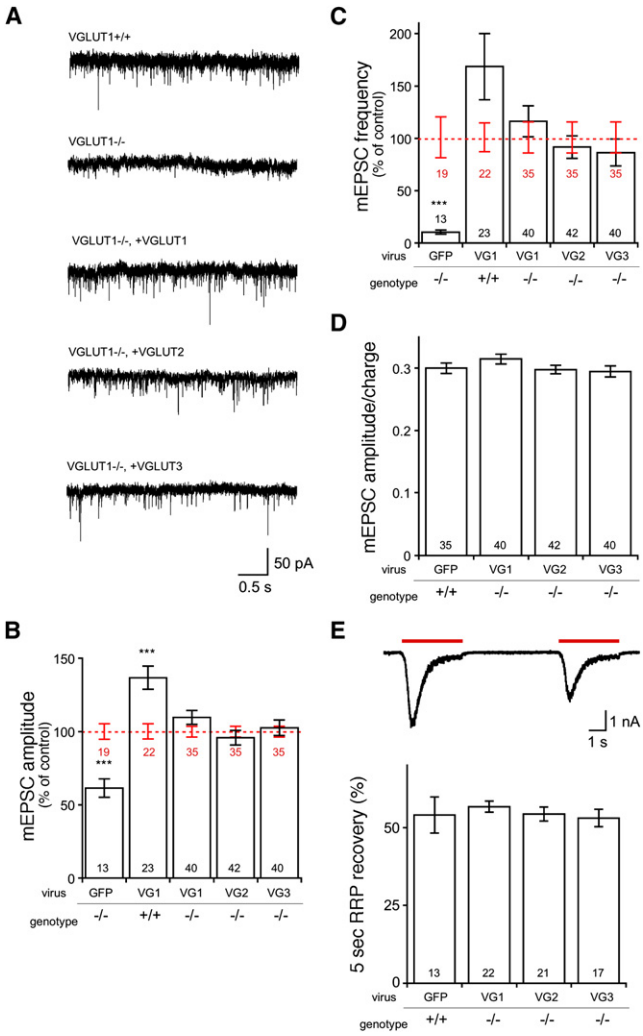

Figure 3. Differences in VGLUT Isoforms Are Not Due to Differences in Spontaneous Release or RRP Refilling

(A) Representative traces showing miniature EPSC (mEPSC) activity in *VGLUT1*+/+, *VGLUT1*−/−, and *VGLUT1*−/− hippocampal neurons rescued with VGLUT1, VGLUT2, or VGLUT3.

(B) Bar graph showing the mEPSC amplitudes recorded from *VGLUT1*−/− neurons, VGLUT1-overexpressing neurons (+/+VG1), and *VGLUT1*−/− rescue neurons. Values (mean ± SEM) are normalized to the mEPSC amplitude of *VGLUT1*+/+ neurons from the same cultures, represented by the red dashed line.

(C) Bar graph showing the mEPSC frequencies recorded from *VGLUT1*−/−, VGLUT1-overexpressing neurons, and *VGLUT1*−/− rescue neurons. Values (mean ± SEM) are normalized to the mEPSC frequency of *VGLUT1*+/+ neurons from the same cultures (red dotted line). Black numbers in bars in both (B) and (C) are n values for experimental groups and red numbers are n values for the control group.

(D) Bar graph showing the ratio of the mEPSC amplitude to the mEPSC charge for *VGLUT1*+/+ neurons and *VGLUT1*−/− rescue neurons (mean ± SEM).

(E) Representative trace of paired sucrose application used to assess pool refilling (top) and bar graph (bottom) showing the percentage of the RRP refilled 5 s after pool depletion by 500 mM sucrose application in *VGLUT1*+/+ neurons and *VGLUT1*−/− rescue neurons (mean ± SEM).

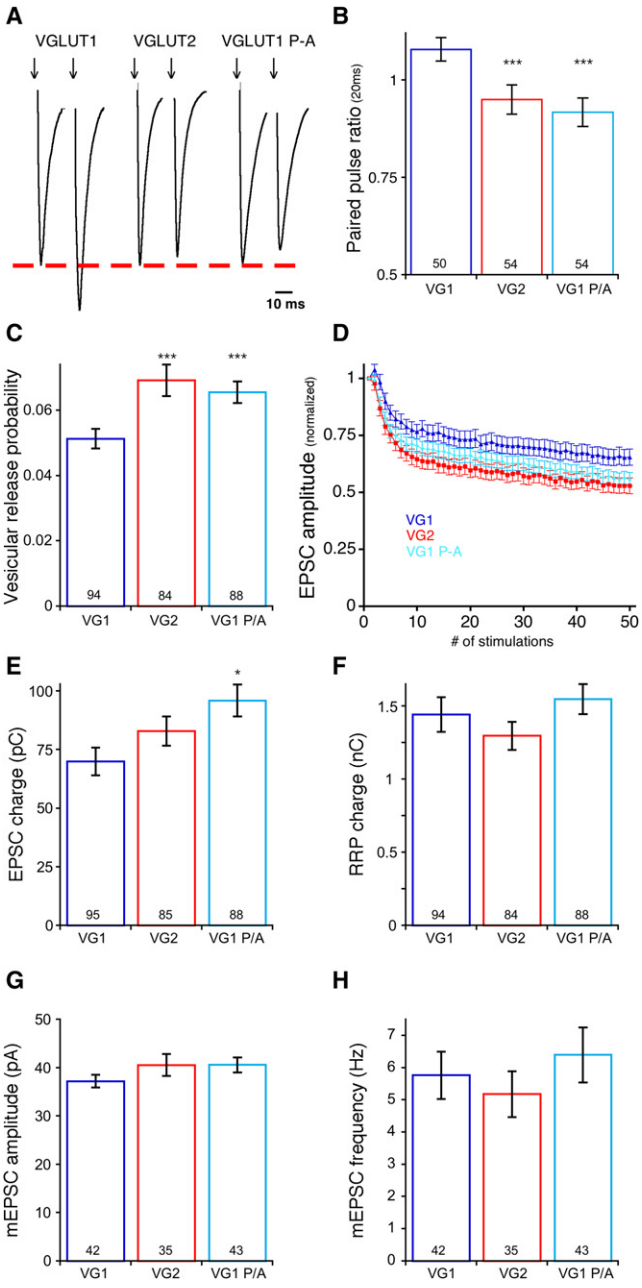

Figure 4. Disruption of VGLUT1-Endophilin Interaction Abolishes Differences in VGLUT Isoforms

(A) Representative paired-pulse EPSC traces from *VGLUT1*−/− hippocampal neurons infected with a VGLUT1-expressing lentivirus (left trace), VGLUT2-expressing lentivirus (middle trace), or VGLUT1 P554A mutant-expressing lentivirus (right trace). Somatic currents are blanked.

(B) Bar graph showing the paired-pulse ratios (mean ± SEM, 20 ms interstimulus interval) measured in *VGLUT1*−/− hippocampal neurons expressing VGLUT1, VGLUT2, or VGLUT1 P554A.

(C) Bar graph showing P_{vr} values measured from *VGLUT1*−/− hippocampal neurons rescued with VGLUT1, VGLUT2, or VGLUT1 P554A (mean ± SEM).

(D) Line plot of the responses of *VGLUT1*−/− hippocampal neurons rescued with VGLUT1, VGLUT2, or VGLUT1 P554A (mean ± SEM) to 10 Hz stimulation. Values are normalized to the peak amplitude of the first response of each neuron.

(E) Bar graph showing EPSC charge measured from *VGLUT1*−/− hippocampal neurons rescued with VGLUT1, VGLUT2, or VGLUT1 P554A (mean ± SEM).

(F) Bar graph showing charge of the RRP measured from *VGLUT1*−/− hippocampal neurons rescued with VGLUT1, VGLUT2, or VGLUT1 P554A (mean ± SEM).

(G) Bar graph showing mEPSC amplitudes measured from *VGLUT1*−/− hippocampal neurons rescued with VGLUT1, VGLUT2, or VGLUT1 P554A (mean ± SEM).

(H) Bar graph showing mEPSC frequency values measured from *VGLUT1*−/− hippocampal neurons rescued with VGLUT1, VGLUT2, or VGLUT1 P554A (mean ± SEM). For all bar graphs *p ≤ 0.05, ***p ≤ 0.001. Numbers in bars are n values.

We found that VGLUT1 P554A induced paired-pulse depression comparable to that observed in VGLUT2-expressing neurons, while VGLUT1 neurons showed facilitation (Figures 4A and 4B). The release probability analysis revealed a 40% increase in P_{vr} in both VGLUT1 P554A- and VGLUT2-expressing neurons compared to VGLUT1 (Figure 4C). VGLUT1 P554A also increased the amount of steady-state depression in response to 10 Hz stimulation from VGLUT1 levels to VGLUT2 levels (Figure 4D). These changes were accompanied by an increase in the charge contained in the EPSC of VGLUT1 P554A-expressing neurons, while the size of the RRP was not different between the three groups (Figures 4E and 4F). mEPSC amplitudes and frequency of VGLUT1 P554A-expressing neurons were not significantly different from VGLUT1- or VGLUT2-expressing neurons (Figures 4G and 4H).

Endophilin Levels Regulate P_{vr} and Short-Term Plasticity Overexpression

Endophilin is a protein that has been implicated in endocytosis and vesicle cycling, so how the interaction of VGLUT1 with endophilin could lower the probability that a vesicle is released in response to an action potential is unclear. We considered two possible mechanisms. First, VGLUT and endophilin may work together to promote a lower P_{vr} for synaptic vesicles on which the complex is present. This could be achieved, for example, if endophilin recruited VGLUT1-containing vesicles to a specific endocytosis pathway (Voglmaier and Edwards, 2007), which could influence the protein composition of synaptic vesicles and therefore their P_{vr}. Second, endophilin alone may promote a higher P_{vr}, possibly by altering vesicle curvature or cargo (Farsad et al., 2001; Gallop et al., 2006; Masuda et al., 2006), and the binding of VGLUT1 may inhibit this function, thus lowering the fusion efficiency of VGLUT1-containing vesicles. To test these two possibilities we overexpressed endophilin in wild-type hippocampal neurons, reasoning that if the first alternative were correct overexpressing endophilin would lower the P_{vr} by binding more VGLUT1. If the second alternative were correct, however, increasing endophilin levels should overwhelm VGLUT1 binding, resulting in more free endophilin and higher P_{vr}. Overexpression of endophilin in wild-type hippocampal neurons was sufficient to raise the P_{vr}, by 50% versus control neurons infected with an RFP-expressing lentivirus. Paired-pulse ratios were decreased by 25% and the extent of depression in response to 10 Hz stimulation was increased by 35%

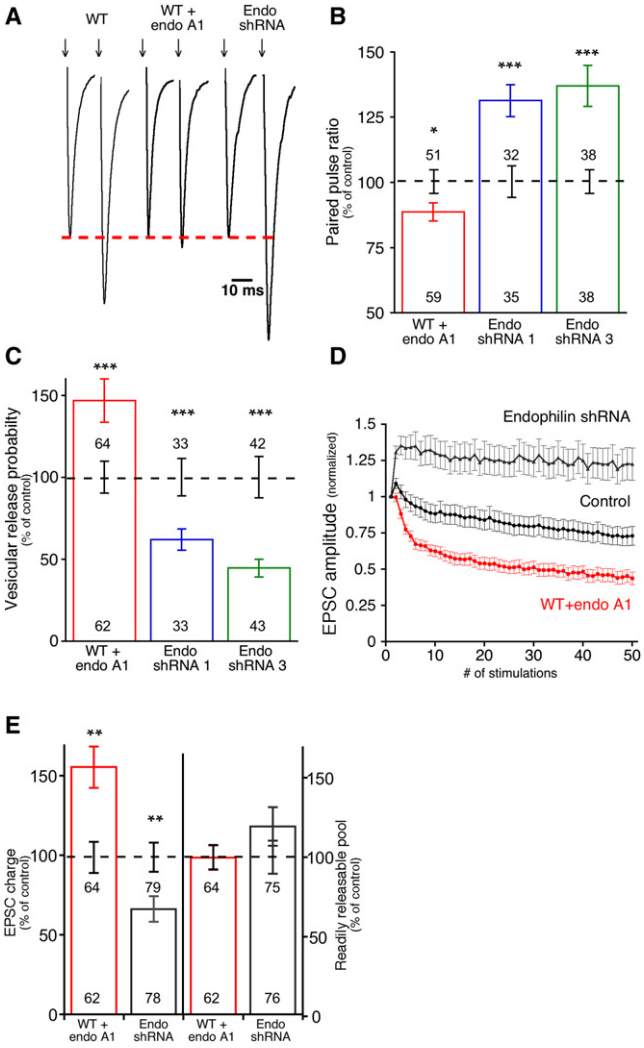

Figure 5. Endophilin A1 Levels Regulate Release Probability and Short-Term Plasticity

(A) Representative paired-pulse EPSC traces from a control neuron (left trace), endophilin A1-overexpressing neuron (middle trace), and endophilin A1 knockdown neuron (right trace).

(B) Bar graph showing the paired-pulse ratios (mean ± SEM, 20 ms interstimulus interval) measured in endophilin A1-overexpressing neurons and neurons expressing two different shRNAs targeting endophilin A1. Data are shown as a percentage of each group's control, which was a lentivirus expressing RFP alone for endophilin overexpression and a lentivirus expressing a shRNA against GFP for the knockdown experiments.

(C) Bar graph showing the P_{vr} (mean ± SEM) measured in endophilin A1-overexpressing neurons and neurons expressing two different shRNAs targeting endophilin A1. Data are shown as a percentage of each group's control.

(D) Line plot of the responses of endophilin A1-overexpressing neurons (red) and endophilin A1 knockdown neurons (gray) to 10 Hz stimulation (mean ± SEM). Values are normalized to the peak amplitude of the first response of each neuron. The endophilin shRNA group is a combination of both shRNAs and the control trace is a combination of control neurons from both shRNA and endophilin overexpression groups for display purposes.

(E) Bar graph showing the charge contained in the EPSC of endophilin A1-overexpressing neurons (red) and endophilin A1 knockdown neurons (gray) on the left and the charge contained in the RRP as measured by the charge transfer in response to a 4 s application of 500 mM sucrose on the right. Data are shown as a percentage of each group's control, represented by the black dashed line (mean ± SEM). For all bar graphs *p ≤ 0.05, **p ≤ 0.01, ***p ≤ 0.001. Lower numbers in bars are n values for experimental groups and upper numbers are n values for control groups.

versus wild-type neurons (Figures 5A–5D). Accompanying the increase in P_{vr}, the EPSC charge increased by approximately 50%, while there was no change in RRP size (Figure 5E). Western blot analysis indicated that the level of endophilin expression was increased approximately 2-fold (Figure S2A).

Knockdown

If, as the results of the endophilin overexpression experiments suggest, endophilin itself exerts a positive effect on the fusion efficiency of vesicles, then reducing the levels of endophilin in the neuron might lower release efficiency. To test this we infected neurons with lentiviruses expressing shRNAs to knock down endophilin A1 and compared them to neurons infected with a lentivirus expressing nonspecific shRNAs. We used western blot analysis to screen several shRNAs and selected two that reduced the level of endophilin A1 expression by 75%–90% (Figure S2B). Analysis of neurons infected with either of the two hairpins showed that reduction in the levels of endophilin A1 protein caused a 50% reduction in P_{vr}. Paired-pulse ratios were increased by 50% and the depression in response to 10 Hz stimulation seen in control neurons was converted to facilitation (Figures 5A–5D). The EPSC charge decreased by approximately 40%, but there was no change in RRP size (Figure 5E).

Membrane Binding and Dimerization, but Not the SH3 Domain, Are Required for Endophilin's Enhancement of Release Efficiency

To further investigate the mechanism of endophilin A1's effect on release efficiency we performed a structure-function analysis. We created three endophilin A1 mutations (Figure 6A). The first was a deletion of the SH3 domain that mediates interactions with proteins such as dynamin, synaptojanin, and VGLUT1 (Cestra et al., 1999; Gad et al., 2000; Schmidt et al., 1999; Vinatier et al., 2006). The second was a deletion of the helix 1 insert shown to disrupt endophilin dimer formation and the third was a KKK-EEE mutation at the BAR domain tips shown to disrupt endophilin's membrane binding properties (Gallop et al., 2006; Mizuno et al., 2010). We overexpressed each of these mutants on the wild-type background and compared their effects on P_{vr} and short-term plasticity to the effects of wild-type endophilin A1. Neurons overexpressing either the KKK-EEE mutation or the helix 1 insert deletion were not significantly different from wild-type neurons infected with an RFP-expressing lentivirus (Figures 6B–6D), suggesting that endophilin's positive effect on release efficiency depends on both membrane binding and dimerization. Overexpression of endophilin lacking the SH3 domain, however, increased P_{vr} and decreased 10 Hz depression to the same extent as wild-type endophilin (Figures 6B and 6C). The EPSC charge of neurons overexpressing the SH3 deletion mutant was significantly greater than controls, but the RRP size was not changed (Figures 6E and 6F). Paired-pulse

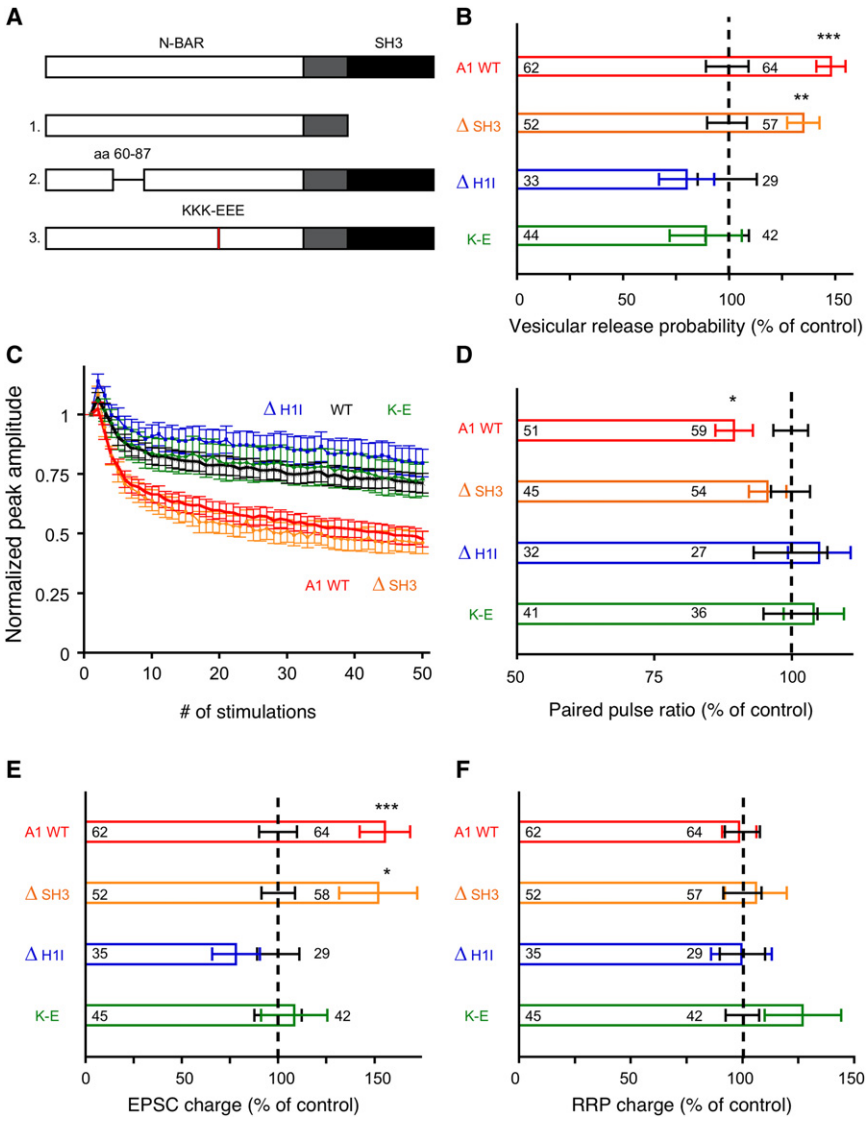

Figure 6. Endophilin Enhancement of Release Probability Requires Membrane Binding and Dimerization but Not the SH3 Domain

(A) Domain diagrams of wild-type endophilin A1 (top) and mutants showing the N-BAR domain (white), variable region (gray), and the SH3 domain (black). The mutations are: (1) deletion of the SH3 domain; (2) deletion of the helix 1 insert in the N-BAR domain; (3) a triple lysine to glutamate substitution at the tips of the N-BAR domain.

(B) Bar graph showing the P_{vr} (mean ± SEM) measured in endophilin A1-overexpressing neurons (red) and neurons overexpressing the endophilin A1 SH3 domain deletion (orange), the helix 1 insert deletion (blue), and the lysine to glutamate substitution at the tips of the BAR domain (green). Data are shown as a percentage of each group's internal control because of the large number of groups.

(C) Line plot of the responses of wild-type, endophilin A1-overexpressing neurons, and endophilin A1 mutant neurons to 10 Hz stimulation (mean ± SEM). Values are normalized to the peak amplitude of the first response of each neuron.

(D) Bar graph showing the paired-pulse ratios (mean ± SEM, 20 ms interstimulus interval) measured in wild-type, endophilin A1-overexpressing neurons, and endophilin A1 mutant neurons. Data are shown as a percentage of each group's internal control.

(E) Bar graph showing the EPSC charge values (mean ± SEM) measured in wild-type, endophilin A1-overexpressing neurons, and endophilin A1 mutant neurons.

(F) Bar graph showing the RRP charge values (mean ± SEM) measured in wild-type, endophilin A1-overexpressing neurons, and endophilin A1 mutant neurons. For all bar graphs *$p \leq 0.05$, **$p \leq 0.01$,***$p \leq 0.001$. Leftmost numbers in bars are n values for experimental groups and rightmost numbers are n values for control groups.

ratios were not significantly decreased (Figure 6D). Thus, endophilin's positive effect on exocytosis is probably independent of its interactions with dynamin, synaptojanin, or VGLUT1.

VGLUT1 Lowers Release Probability by Binding and Blocking Endophilin's Enhancement of Release Efficiency

To ensure that the lower release probability of VGLUT1-expressing cells was a direct result of VGLUT1 binding and inhibiting endophilin A1, we took advantage of the fact that both the full-length endophilin A1 and the SH3 deletion mutant were sufficient to raise release probability in control cells. If VGLUT1 indeed binds endophilin and inhibits its ability to raise release probability, then overexpressing VGLUT1 should prevent any endophilin A1-induced increase in release probability, but have no effect on the endophilin SH3 deletion mutant's increase in release probability, because of the inability of VGLUT1 to bind endophilin in the absence of the SH3 domain. We therefore compared neurons overexpressing VGLUT1 and endophilin A1 and neurons overexpressing VGLUT1 and the endophilin A1 SH3 deletion with control neurons. We found that overexpression of VGLUT1 was sufficient to block the increase in release probability normally caused by endophilin overexpression (Figure 7A). However, overexpression of VGLUT1 did not block the increase in release probability caused by the endophilin SH3 deletion mutant, demonstrating that VGLUT1's ability to lower release probability is dependent on binding of endophilin A1 (Figures 7A and 7B). There were no significant changes in EPSC charge or RRP size (Figure 7C).

As a final test of our hypothesis that the lower release probability of VGLUT1-expressing neurons is due to VGLUT1's ability to bind and inhibit endophilin, we introduced the endophilin binding domain of VGLUT1 into VGLUT2 by replacing the carboxy-terminal amino acids of VGLUT2 (502–582) with

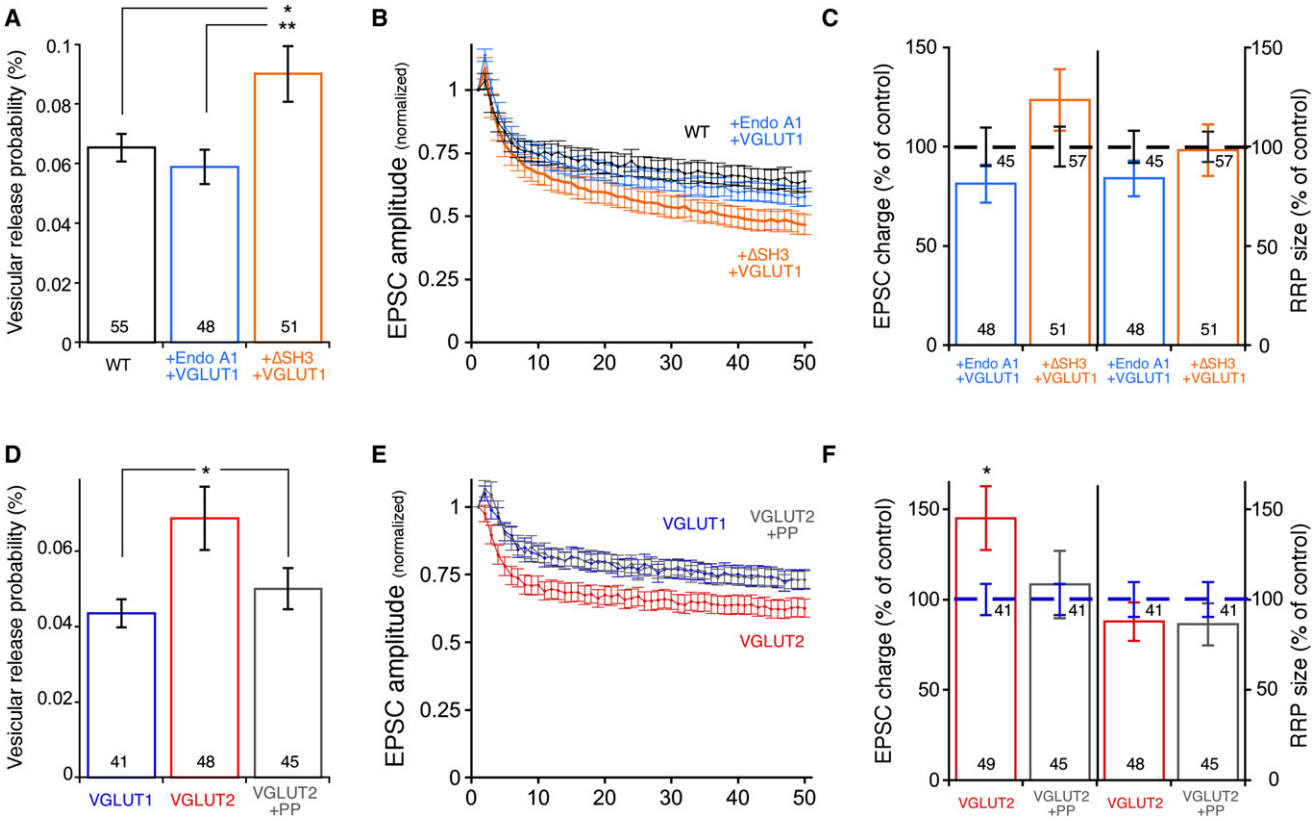

Figure 7. The Polyproline Motif of VGLUT1 Lowers Release Probability by Binding and Blocking Endophilin A1 Activity

(A) Bar graph showing the P_{vr} (mean ± SEM) measured in wild-type neurons (black), neurons overexpressing endophilin A1 and VGLUT1 (blue), and neurons overexpressing the SH3 domain deletion and VGLUT1 (orange).

(B) Line plot of the responses of wild-type neurons (black), neurons overexpressing endophilin A1 and VGLUT1 (blue), and neurons overexpressing the endophilin A1 SH3 domain deletion mutant and VGLUT1 (orange) to 10 Hz stimulation (mean ± SEM). Values are normalized to the peak amplitude of the first response of each neuron.

(C) Bar graph of the EPSC charge (left bars) and RRP charge (right bars) from neurons overexpressing endophilin A1 and VGLUT1 (blue) and neurons overexpressing the endophilin A1 SH3 domain deletion mutant and VGLUT1 (orange). Data are shown as a percentage of each group's internal control, represented by the black dashed line.

(D) Bar graph showing the P_{vr} (mean ± SEM) measured in *VGLUT1*−/− neurons expressing VGLUT1 (blue), VGLUT2 (red), or VGLUT2 with the VGLUT1 C-terminal region containing the polyproline motif (gray).

(E) Line plot of the responses from *VGLUT1*−/− neurons expressing VGLUT1 (blue), VGLUT2 (red), or VGLUT2 with the VGLUT1 C-terminal region containing the polyproline motif (gray). Values are normalized to the peak amplitude of the first response of each neuron.

(F) Bar graph of the EPSC charge (left bars) and RRP charge (right bars) from VGLUT2 (red) or VGLUT2 with the VGLUT1 C-terminal region containing the polyproline motif (gray). Data are shown as a percentage of the mean of VGLUT1-expressing neurons, represented by the blue dotted line. *$p \leq 0.05$, **$p \leq 0.01$. Lower numbers in bar graph are n values for experimental groups and upper numbers are n values for control groups.

amino acids 494–560 of VGLUT1. We then compared this mutant's rescue activity to wild-type VGLUT1 and VGLUT2 in the *VGLUT1*−/− hippocampal neuron background. Once again, VGLUT2-expressing neurons had higher P_{vr} and more depression in response to 10 Hz stimulation than VGLUT1-expressing neurons (Figures 7D and 7E). The VGLUT2 mutant, however, had P_{vr} that was not different from VGLUT1 but significantly lower than VGLUT2, with concomitant changes in 10 Hz stimulation (Figures 7D and 7E). In this set of experiments VGLUT2-expressing neurons had a significantly larger EPSC charge than VGLUT1- or VGLUT2-mutant-expressing neurons, while the RRP size was not different among the groups (Figure 7F).

DISCUSSION

The central nervous system processes a large variety of information, including sensory processing and motor control, body homeostasis, emotions, and higher cognitive functions, within hundreds of anatomically and functionally distinct circuits. To accomplish this diversity, the neurons and synapses underlying these circuits employ a large set of tools including variation in neuronal morphology, synaptic connectivity, electrical processing within the neuron, and synaptic function. Presynaptic release probabilities are a major contributor to the functional diversity of synapses. They determine both the initial reliability of a synaptic connection and the short-term plasticity

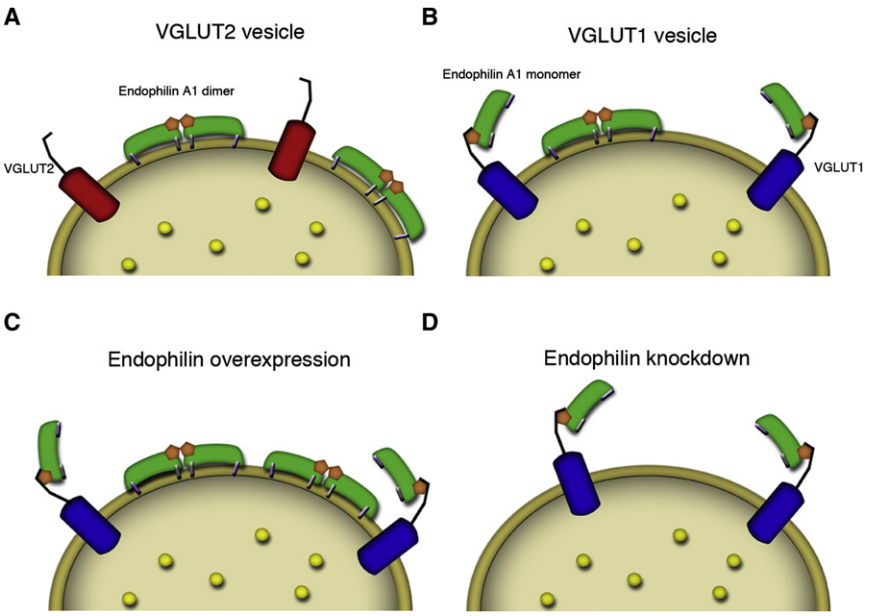

Figure 8. Proposed Model for the Mechanism Underlying VGLUT Isoform Regulation of Release Probability

(A) VGLUT2-containing vesicles, because of the inability of VGLUT2 to bind endophilin, have high levels of active endophilin and therefore have a high P_{vr}.

(B) VGLUT1-containing vesicles, because of VGLUT1 binding endophilin, have lower levels of active endophilin and therefore have a low P_{vr}.

(C) Overexpression of endophilin A1 overwhelms the available VGLUT1 binding sites for endophilin, resulting in higher levels of active endophilin and higher P_{vr}.

(D) Knockdown of endophilin A1 reduces the amount of active endophilin and lowers P_{vr}. As pictured, the model assumes that endophilin A1 in its membrane-bound, dimerized (active) state enhances the fusion probability of individual synaptic vesicles and that VGLUT1 binding to the endophilin SH3 domain (orange pentagons) prevents endophilin membrane binding and/or dimerization.

characteristics, as low-release probability synapses show facilitation, while high-release probability synapses tend to depress during action potential trains. The molecular mechanisms for the diversity of release probability are practically unknown.

Here we demonstrate a molecular mechanism of regulation of release probability that contributes to the functional diversity of different synapse populations. We identify endophilin A1 as a positive regulator of release probability and show how differential expression of VGLUT isoforms in neurons interact with endophilin A1 to shape the synaptic response. We propose the following model for the VGLUT isoforms' regulation of release probability (Figure 8). The model shows that endophilin dimerizes and binds to synaptic vesicle membranes to achieve an active state that enhances release efficiency. This may be a transient state during endocytosis and vesicle formation, or a longer lasting state, and may also occur at the neck of vesicle invaginations. VGLUT2-containing vesicles (top left) have high levels of active endophilin and high-release probability, while VGLUT1-containing vesicles (top right) have lower levels of active endophilin because of the inhibitory actions of VGLUT1. Overexpression of endophilin (bottom left) overwhelms the available VGLUT1 molecules and raises the level of active endophilin and the probability of vesicle release. Knockdown of endophilin (bottom right) severely decreases levels of active endophilin and the probability of vesicle release.

The classical role of VGLUTs is to fill vesicles with glutamate, and therefore the additional role in regulating release probability is surprising. Although it had been noted previously that the distribution of VGLUT1 and VGLUT2 overlaps with that of synapses with different reliability (Fremeau et al., 2001; Liu, 2003), it was difficult to imagine how a vesicular neurotransmitter transporter might cause synapses to release glutamatergic vesicles with different probability. Here we provide a molecular explanation for the correlation between VGLUT expression and release probability. Another important finding is that VGLUT3 expression suffices for the induction of vesicular glutamate uptake and release in nonglutamatergic neurons. While recent data from VGLUT3-deficient neurons demonstrated the necessity of VGLUT3 function for glutamatergic neurotransmission in auditory hair cells and pain pathways (Obholzer et al., 2008; Ruel et al., 2008; Seal et al., 2008, 2009), our demonstration that this effect is a direct result of VGLUT3's ability to function as a classical vesicular transporter is critical in interpreting morphological data showing that VGLUT3 localizes to terminals from serotonergic, cholinergic, and GABAergic neurons. Based on our findings, these synapses are very likely coreleasing glutamate along with their classical neurotransmitters, which implies a fast excitatory signaling component at these classically modulatory synapses.

Previous studies have shown that VGLUT levels are endogenously and bidirectionally regulated during development (Boulland et al., 2004; Nakamura et al., 2005), in disease states (Eastwood and Harrison, 2005; Kashani et al., 2007; Smith et al., 2001), with pharmacological manipulation (De Gois et al., 2005; Wilson et al., 2005), and according to circadian rhythms (Yelamanchili et al., 2006). Our data suggest these alterations would be accompanied by changes in neuronal firing patterns and perhaps circuit behavior. For example, differences between VGLUT1 and VGLUT2/3 could be important during development, where the early, transient expression of VGLUT2 and VGLUT3 in neurons that later express VGLUT1 could increase the chance of glutamate release at synapses that may contain fewer synaptic vesicles than mature synapses. It is possible that neurons or networks of neurons actively use specific VGLUT isoform expression to regulate the efficiency of glutamate release.

The mechanism by which endophilin levels regulate release efficiency is still unknown. Because endophilin is a protein known primarily for its role in endocytosis, it is possible that it acts by altering either the size of the RRP or its rate of replenishment. However, overexpression and knockdown of endophilin

did not affect the RRP. Instead they increased and decreased the EPSC charge, suggesting that endophilin directly alters the fusion efficiency of synaptic vesicles. Because this effect does not require the SH3 domain, it is not likely to involve increased recruitment of dynamin or synaptojanin. The effect is, however, dependent on membrane binding and dimerization. Although it is likely that many of endophilin's actions are dependent on interactions with synaptojanin and dynamin, recent evidence suggests endophilin's main endocytic function requires only the BAR domain and occurs at the plasma membrane prior to vesicle scission (Bai et al., 2010). It is therefore possible that the mechanism by which endophilin promotes endocytosis and enhances release probability are one and the same and that it acts at the step of vesicle retrieval from the plasma membrane to form vesicles that have an intrinsically higher release probability. This could be accomplished by altering the curvature of synaptic vesicles, altering the timing of membrane scission, or altering the internalization of endocytic cargo (Bai et al., 2010; Jao et al., 2010; Suresh and Edwardson, 2010).

EXPERIMENTAL PROCEDURES

Electrophysiology and Cell Culture

Microisland cultures of E17.5 striatal, hippocampal, and thalamic neurons were prepared according to published procedures (Pyott and Rosenmund, 2002). *VGLUT1* knockout mice were described previously (Wojcik et al., 2004). *VGLUT2* knockout mice were also described previously (Moechars et al., 2006). All procedures to maintain and use these mice were approved by the Institutional Animal Care and Use Committee for Baylor College of Medicine and Affiliates. Cultures were plated on astrocytes derived from P1 cortex tissue at a density of 2000–3000 neurons per 35 mm dish. Extracellular solution contained 140 mM NaCl, 2.4 mM KCl, 10 mM HEPES, 10 mM glucose, 4 mM $MgCl_2$, and 2 mM $CaCl_2$, pH 7.3 (305 mOsm). Internal solution contained 136 mM KCl, 17.8 mM HEPES, 1 mM EGTA, 0.6 mM $MgCl_2$, 4 mM ATP, 0.3 mM GTP, 12 mM creatine phosphate, and 50 U/ml phosphocreatine kinase. All experiments were performed at room temperature (23°C–24°C).

Whole-cell voltage-clamp recordings were performed on neurons from control and experimental groups in parallel on the same day (9–14 in vitro). Action potential-evoked EPSCs or IPSCs were triggered by a 2 ms somatic depolarization to 0 mV. RRP size was determined by integrating the transient synaptic current induced by a 4 s application of hypertonic sucrose solution directly onto the neuron. To obtain P_{vr}, we recorded the basal evoked synaptic responses and the response to the hypertonic sucrose solution successively from the same neuron. The evoked response was integrated for 1 s to calculate the charge transfer. P_{vr} was calculated as the ratio of evoked response charge to RRP charge. Short-term plasticity was examined either by evoking 50 synaptic responses at 10 Hz or 2 responses with a 20 ms interval in standard external solution. Data were analyzed offline by using AxoGraph X 1.0 (AxoGraph Scientific, Sydney, Australia) and KaleidaGraph (Synergy Software, Reading, PA). Values for analysis were pooled from at least two independent cultures. Statistical significances were tested by using Student's t test for two groups with normal distribution, the nonparametric Kolmogorov-Smirnov test for two groups that were not normally distributed, or one-way ANOVA with a Student-Newman-Keuls post hoc test for three or more groups. For values reported as normalized, the average value of the control group (either wild-type neurons or neurons rescued with the wild-type isoform) was calculated for each day and then used to normalize individual neuron values from each group for that day.

Miniature EPSC Analysis

mEPSCs were detected for 60–80 s with 3 mM kynurenic acid applied for 2 s of every 10 s for background noise subtraction. For each cell, data were filtered at 1 kHz and analyzed by using template-based mEPSC detection algorithms implemented in AxoGraph X 1.0 (AxoGraph Scientific). The threshold for detection was set at three times the baseline SD from a template of 0.5 ms rise time and 3 ms decay.

Lentivirus Constructs and Production

The preparation of lentiviral particles expressing different VGLUTs was done as described (Lois et al., 2002). Briefly, HEK293T cells were cotransfected with 8 μg shuttle vector F(SYN)UGW-RBN bearing cDNAs for the different VGLUTs and the mixed helper plasmids pCMVdR8.9 and pVSV-G (5 μg each) with Fugene 6 transfection reagent (Roche Diagnostics, Indianapolis, IN). After 48 hr the cell culture supernatant was collected and cell debris was removed by filtration. Aliquots of the filtrate were flash-frozen in liquid nitrogen and stored at −80°C. Estimation of the titer was done on mass cultures of wild-type hippocampal neurons. For infection of the neurons for experiments 300–500 μl of the viral solution (0.9–1.8 × 10^6 IU/ml) was used 18–24 hr after plating.

shRNA Experiments

Five different shRNAs from the TRC-Mm1.0 library targeted against endophilin A1 in the pLKO.1 vector were obtained from Open Biosystems (Huntsville, AL), as well as a control sequence against eGFP. Lentiviral particles were prepared as described above. Estimation of the titer was done on mass cultures of wild-type hippocampal neurons by applying puromycin (2 μg/ml) and counting the numbers of surviving cells after 48 hr. Equal amounts of control and shRNA viral particles (~2 × 10^6 IU) were then applied to mass cultures of hippocampal neurons. After 14 days in vitro cells were harvested and western blot analysis was used to assess the amount of reduction in endophilin A1 protein.

SUPPLEMENTAL INFORMATION

Supplemental Information includes two figures and Supplemental Experimental Procedures and can be found with this article online at doi:10.1016/j.neuron.2011.02.002.

ACKNOWLEDGMENTS

We thank Hongmei Chen for help with mouse care and genotyping, Hui Deng and Marife Arancillo for help with cell culture and virus production, Dieter Moechars for supplying the VGLUT2 knockout mice, Etienne Herzog for supplying endophilin antibodies and cDNA, and Amy Shore for help with molecular cloning and design of Figure 8. This work was supported by a Helen and Rush Record fellowship (M.C.W.), by a Human Frontier Science Program Research Grant, by the European Research Council grant SYNVGLUT, and by the German Research Council Excellence Cluster Neurocure (C.R).

Accepted: January 14, 2011
Published: March 23, 2011

REFERENCES

Amilhon, B., Lepicard, E., Renoir, T., Mongeau, R., Popa, D., Poirel, O., Miot, S., Gras, C., Gardier, A.M., Gallego, J., et al. (2010). VGLUT3 (vesicular glutamate transporter type 3) contribution to the regulation of serotonergic transmission and anxiety. J. Neurosci. *30*, 2198–2210.

Bai, L., Xu, H., Collins, J.F., and Ghishan, F.K. (2001). Molecular and functional analysis of a novel neuronal vesicular glutamate transporter. J. Biol. Chem. *276*, 36764–36769.

Bai, J., Hu, Z., Dittman, J.S., Pym, E.C., and Kaplan, J.M. (2010). Endophilin functions as a membrane-bending molecule and is delivered to endocytic zones by exocytosis. Cell *143*, 430–441.

Bellocchio, E.E., Reimer, R.J., Fremeau, R.T., Jr., and Edwards, R.H. (2000). Uptake of glutamate into synaptic vesicles by an inorganic phosphate transporter. Science *289*, 957–960.

Boulland, J.L., Qureshi, T., Seal, R.P., Rafiki, A., Gundersen, V., Bergersen, L.H., Fremeau, R.T., Jr., Edwards, R.H., Storm-Mathisen, J., and Chaudhry, F.A. (2004). Expression of the vesicular glutamate transporters during

development indicates the widespread corelease of multiple neurotransmitters. J. Comp. Neurol. *480*, 264–280.

Cestra, G., Castagnoli, L., Dente, L., Minenkova, O., Petrelli, A., Migone, N., Hoffmüller, U., Schneider-Mergener, J., and Cesareni, G. (1999). The SH3 domains of endophilin and amphiphysin bind to the proline-rich region of synaptojanin 1 at distinct sites that display an unconventional binding specificity. J. Biol. Chem. *274*, 32001–32007.

De Gois, S., Schäfer, M.K., Defamie, N., Chen, C., Ricci, A., Weihe, E., Varoqui, H., and Erickson, J.D. (2005). Homeostatic scaling of vesicular glutamate and GABA transporter expression in rat neocortical circuits. J. Neurosci. *25*, 7121–7133.

De Gois, S., Jeanclos, E., Morris, M., Grewal, S., Varoqui, H., and Erickson, J.D. (2006). Identification of endophilins 1 and 3 as selective binding partners for VGLUT1 and their co-localization in neocortical glutamatergic synapses: Implications for vesicular glutamate transporter trafficking and excitatory vesicle formation. Cell. Mol. Neurobiol. *26*, 679–693.

Eastwood, S.L., and Harrison, P.J. (2005). Decreased expression of vesicular glutamate transporter 1 and complexin II mRNAs in schizophrenia: Further evidence for a synaptic pathology affecting glutamate neurons. Schizophr. Res. *73*, 159–172.

Farsad, K., Ringstad, N., Takei, K., Floyd, S.R., Rose, K., and De Camilli, P. (2001). Generation of high curvature membranes mediated by direct endophilin bilayer interactions. J. Cell Biol. *155*, 193–200.

Fremeau, R.T., Jr., Troyer, M.D., Pahner, I., Nygaard, G.O., Tran, C.H., Reimer, R.J., Bellocchio, E.E., Fortin, D., Storm-Mathisen, J., and Edwards, R.H. (2001). The expression of vesicular glutamate transporters defines two classes of excitatory synapse. Neuron *31*, 247–260.

Fremeau, R.T., Jr., Kam, K., Qureshi, T., Johnson, J., Copenhagen, D.R., Storm-Mathisen, J., Chaudhry, F.A., Nicoll, R.A., and Edwards, R.H. (2004). Vesicular glutamate transporters 1 and 2 target to functionally distinct synaptic release sites. Science *304*, 1815–1819.

Gad, H., Ringstad, N., Löw, P., Kjaerulff, O., Gustafsson, J., Wenk, M., Di Paolo, G., Nemoto, Y., Crun, J., Ellisman, M.H., et al. (2000). Fission and uncoating of synaptic clathrin-coated vesicles are perturbed by disruption of interactions with the SH3 domain of endophilin. Neuron *27*, 301–312.

Gallop, J.L., Jao, C.C., Kent, H.M., Butler, P.J., Evans, P.R., Langen, R., and McMahon, H.T. (2006). Mechanism of endophilin N-BAR domain-mediated membrane curvature. EMBO J. *25*, 2898–2910.

Gillespie, D.C., Kim, G., and Kandler, K. (2005). Inhibitory synapses in the developing auditory system are glutamatergic. Nat. Neurosci. *8*, 332–338.

Gras, C., Herzog, E., Bellenchi, G.C., Bernard, V., Ravassard, P., Pohl, M., Gasnier, B., Giros, B., and El Mestikawy, S. (2002). A third vesicular glutamate transporter expressed by cholinergic and serotoninergic neurons. J. Neurosci. *22*, 5442–5451.

Gras, C., Amilhon, B., Lepicard, E.M., Poirel, O., Vinatier, J., Herbin, M., Dumas, S., Tzavara, E.T., Wade, M.R., Nomikos, G.G., et al. (2008). The vesicular glutamate transporter VGLUT3 synergizes striatal acetylcholine tone. Nat. Neurosci. *11*, 292–300.

Guichet, A., Wucherpfennig, T., Dudu, V., Etter, S., Wilsch-Bräuniger, M., Hellwig, A., González-Gaitán, M., Huttner, W.B., and Schmidt, A.A. (2002). Essential role of endophilin A in synaptic vesicle budding at the Drosophila neuromuscular junction. EMBO J. *21*, 1661–1672.

Hayashi, M., Otsuka, M., Morimoto, R., Hirota, S., Yatsushiro, S., Takeda, J., Yamamoto, A., and Moriyama, Y. (2001). Differentiation-associated Na+-dependent inorganic phosphate cotransporter (DNPI) is a vesicular glutamate transporter in endocrine glutamatergic systems. J. Biol. Chem. *276*, 43400–43406.

Herzog, E., Bellenchi, G.C., Gras, C., Bernard, V., Ravassard, P., Bedet, C., Gasnier, B., Giros, B., and El Mestikawy, S. (2001). The existence of a second vesicular glutamate transporter specifies subpopulations of glutamatergic neurons. J. Neurosci. *21*, RC181.

Herzog, E., Gilchrist, J., Gras, C., Muzerelle, A., Ravassard, P., Giros, B., Gaspar, P., and El Mestikawy, S. (2004). Localization of VGLUT3, the vesicular glutamate transporter type 3, in the rat brain. Neuroscience *123*, 983–1002.

Hill, E., van Der Kaay, J., Downes, C.P., and Smythe, E. (2001). The role of dynamin and its binding partners in coated pit invagination and scission. J. Cell Biol. *152*, 309–323.

Jao, C.C., Hegde, B.G., Gallop, J.L., Hegde, P.B., McMahon, H.T., Haworth, I.S., and Langen, R. (2010). Roles of amphipathic helices and the bin/amphiphysin/rvs (BAR) domain of endophilin in membrane curvature generation. J. Biol. Chem. *285*, 20164–20170.

Kaneko, T., and Fujiyama, F. (2002). Complementary distribution of vesicular glutamate transporters in the central nervous system. Neurosci. Res. *42*, 243–250.

Kaneko, T., Fujiyama, F., and Hioki, H. (2002). Immunohistochemical localization of candidates for vesicular glutamate transporters in the rat brain. J. Comp. Neurol. *444*, 39–62.

Kashani, A., Betancur, C., Giros, B., Hirsch, E., and El Mestikawy, S. (2007). Altered expression of vesicular glutamate transporters VGLUT1 and VGLUT2 in Parkinson disease. Neurobiol. Aging *28*, 568–578.

Liu, G. (2003). Presynaptic control of quantal size: Kinetic mechanisms and implications for synaptic transmission and plasticity. Curr. Opin. Neurobiol. *13*, 324–331.

Lois, C., Hong, E.J., Pease, S., Brown, E.J., and Baltimore, D. (2002). Germline transmission and tissue-specific expression of transgenes delivered by lentiviral vectors. Science *295*, 868–872.

Masuda, M., Takeda, S., Sone, M., Ohki, T., Mori, H., Kamioka, Y., and Mochizuki, N. (2006). Endophilin BAR domain drives membrane curvature by two newly identified structure-based mechanisms. EMBO J. *25*, 2889–2897.

Mizuno, N., Jao, C.C., Langen, R., and Steven, A.C. (2010). Multiple modes of endophilin-mediated conversion of lipid vesicles into coated tubes: Implications for synaptic endocytosis. J. Biol. Chem. *285*, 23351–23358.

Moechars, D., Weston, M.C., Leo, S., Callaerts-Vegh, Z., Goris, I., Daneels, G., Buist, A., Cik, M., van der Spek, P., Kass, S., et al. (2006). Vesicular glutamate transporter VGLUT2 expression levels control quantal size and neuropathic pain. J. Neurosci. *26*, 12055–12066.

Nakamura, K., Hioki, H., Fujiyama, F., and Kaneko, T. (2005). Postnatal changes of vesicular glutamate transporter (VGluT)1 and VGluT2 immunoreactivities and their colocalization in the mouse forebrain. J. Comp. Neurol. *492*, 263–288.

Obholzer, N., Wolfson, S., Trapani, J.G., Mo, W., Nechiporuk, A., Busch-Nentwich, E., Seiler, C., Sidi, S., Söllner, C., Duncan, R.N., et al. (2008). Vesicular glutamate transporter 3 is required for synaptic transmission in zebrafish hair cells. J. Neurosci. *28*, 2110–2118.

Pyott, S.J., and Rosenmund, C. (2002). The effects of temperature on vesicular supply and release in autaptic cultures of rat and mouse hippocampal neurons. J. Physiol. *539*, 523–535.

Ringstad, N., Gad, H., Löw, P., Di Paolo, G., Brodin, L., Shupliakov, O., and De Camilli, P. (1999). Endophilin/SH3p4 is required for the transition from early to late stages in clathrin-mediated synaptic vesicle endocytosis. Neuron *24*, 143–154.

Rosenmund, C., and Stevens, C.F. (1996). Definition of the readily releasable pool of vesicles at hippocampal synapses. Neuron *16*, 1197–1207.

Ruel, J., Emery, S., Nouvian, R., Bersot, T., Amilhon, B., Van Rybroek, J.M., Rebillard, G., Lenoir, M., Eybalin, M., Delprat, B., et al. (2008). Impairment of SLC17A8 encoding vesicular glutamate transporter-3, VGLUT3, underlies nonsyndromic deafness DFNA25 and inner hair cell dysfunction in null mice. Am. J. Hum. Genet. *83*, 278–292.

Schäfer, M.K., Varoqui, H., Defamie, N., Weihe, E., and Erickson, J.D. (2002). Molecular cloning and functional identification of mouse vesicular glutamate transporter 3 and its expression in subsets of novel excitatory neurons. J. Biol. Chem. *277*, 50734–50748.

Schmidt, A., Wolde, M., Thiele, C., Fest, W., Kratzin, H., Podtelejnikov, A.V., Witke, W., Huttner, W.B., and Söling, H.D. (1999). Endophilin I mediates

synaptic vesicle formation by transfer of arachidonate to lysophosphatidic acid. Nature *401*, 133–141.

Schuske, K.R., Richmond, J.E., Matthies, D.S., Davis, W.S., Runz, S., Rube, D.A., van der Bliek, A.M., and Jorgensen, E.M. (2003). Endophilin is required for synaptic vesicle endocytosis by localizing synaptojanin. Neuron *40*, 749–762.

Seal, R.P., Akil, O., Yi, E., Weber, C.M., Grant, L., Yoo, J., Clause, A., Kandler, K., Noebels, J.L., Glowatzki, E., et al. (2008). Sensorineural deafness and seizures in mice lacking vesicular glutamate transporter 3. Neuron *57*, 263–275.

Seal, R.P., Wang, X., Guan, Y., Raja, S.N., Woodbury, C.J., Basbaum, A.I., and Edwards, R.H. (2009). Injury-induced mechanical hypersensitivity requires C-low threshold mechanoreceptors. Nature *462*, 651–655.

Simpson, F., Hussain, N.K., Qualmann, B., Kelly, R.B., Kay, B.K., McPherson, P.S., and Schmid, S.L. (1999). SH3-domain-containing proteins function at distinct steps in clathrin-coated vesicle formation. Nat. Cell Biol. *1*, 119–124.

Smith, R.E., Haroutunian, V., Davis, K.L., and Meador-Woodruff, J.H. (2001). Vesicular glutamate transporter transcript expression in the thalamus in schizophrenia. Neuroreport *12*, 2885–2887.

Suresh, S., and Edwardson, J.M. (2010). The endophilin N-BAR domain perturbs the structure of lipid bilayers. Biochemistry *49*, 5766–5771.

Takamori, S., Rhee, J.S., Rosenmund, C., and Jahn, R. (2000). Identification of a vesicular glutamate transporter that defines a glutamatergic phenotype in neurons. Nature *407*, 189–194.

Takamori, S., Rhee, J.S., Rosenmund, C., and Jahn, R. (2001). Identification of differentiation-associated brain-specific phosphate transporter as a second vesicular glutamate transporter (VGLUT2). J. Neurosci. *21*, RC182.

Takamori, S., Malherbe, P., Broger, C., and Jahn, R. (2002). Molecular cloning and functional characterization of human vesicular glutamate transporter 3. EMBO Rep. *3*, 798–803.

Varoqui, H., Schäfer, M.K., Zhu, H., Weihe, E., and Erickson, J.D. (2002). Identification of the differentiation-associated Na+/PI transporter as a novel vesicular glutamate transporter expressed in a distinct set of glutamatergic synapses. J. Neurosci. *22*, 142–155.

Vinatier, J., Herzog, E., Plamont, M.A., Wojcik, S.M., Schmidt, A., Brose, N., Daviet, L., El Mestikawy, S., and Giros, B. (2006). Interaction between the vesicular glutamate transporter type 1 and endophilin A1, a protein essential for endocytosis. J. Neurochem. *97*, 1111–1125.

Voglmaier, S.M., and Edwards, R.H. (2007). Do different endocytic pathways make different synaptic vesicles? Curr. Opin. Neurobiol. *17*, 374–380.

Voglmaier, S.M., Kam, K., Yang, H., Fortin, D.L., Hua, Z., Nicoll, R.A., and Edwards, R.H. (2006). Distinct endocytic pathways control the rate and extent of synaptic vesicle protein recycling. Neuron *51*, 71–84.

Wallén-Mackenzie, A., Gezelius, H., Thoby-Brisson, M., Nygård, A., Enjin, A., Fujiyama, F., Fortin, G., and Kullander, K. (2006). Vesicular glutamate transporter 2 is required for central respiratory rhythm generation but not for locomotor central pattern generation. J. Neurosci. *26*, 12294–12307.

Wilson, N.R., Kang, J., Hueske, E.V., Leung, T., Varoqui, H., Murnick, J.G., Erickson, J.D., and Liu, G. (2005). Presynaptic regulation of quantal size by the vesicular glutamate transporter VGLUT1. J. Neurosci. *25*, 6221–6234.

Wojcik, S.M., Rhee, J.S., Herzog, E., Sigler, A., Jahn, R., Takamori, S., Brose, N., and Rosenmund, C. (2004). An essential role for vesicular glutamate transporter 1 (VGLUT1) in postnatal development and control of quantal size. Proc. Natl. Acad. Sci. USA *101*, 7158–7163.

Yelamanchili, S.V., Pendyala, G., Brunk, I., Darna, M., Albrecht, U., and Ahnert-Hilger, G. (2006). Differential sorting of the vesicular glutamate transporter 1 into a defined vesicular pool is regulated by light signaling involving the clock gene Period2. J. Biol. Chem. *281*, 15671–15679.